

## Stark magnetophonon resonances in Wannier-Stark localized InAs/GaSb superlattices

R. S. Deacon,\* R. J. Nicholas, and P. A. Shields

Clarendon Laboratory, University of Oxford, Parks Road, Oxford OX1 3PU, United Kingdom

(Received 4 July 2006; published 29 September 2006)

We report an experimental study of high electric field magnetoconduction in semiconducting InAs/GaSb superlattices. This demonstrates that total quantization of the electronic states leads to conduction dominated by a combination of interwell and intrawell processes. The strongest conduction occurs for the triple Stark magnetophonon resonance where resonant interwell tunnelling coincides with (multiple) intrawell longitudinal optical phonon emission.

DOI: 10.1103/PhysRevB.74.121306

PACS number(s): 72.10.Di, 72.80.Ey

Semiconductor superlattices (SLs) comprise alternating layers of two or more semiconductor materials. In an unperturbed superlattice strong coupling between energy levels in adjacent wells results in delocalized wave functions leading to the formation of minibands. The study of electron transport in superlattices<sup>1</sup> has been a active research area since their conception<sup>2</sup> in 1970.

Superlattice transport at low temperatures is characterized by two regimes. At low electric fields where  $\hbar\Omega = eFd \ll \Delta$  (where  $\Omega$  is the Bloch frequency,  $F$  the electric field,  $d$  the superlattice period and  $\Delta$  the miniband width) coherent miniband transport dominates.<sup>3,4</sup> At high electric fields however  $\hbar\Omega > \Delta$  causing the miniband to split into localized Wannier-Stark-ladder (WSL) states<sup>5-7</sup> and consequently miniband transport is no longer the dominant process. Within this regime transport is dominated by scattering mediated hopping transitions between WSL states<sup>8</sup> and energy loss mechanisms become paramount in determining the current flow. The spatial overlap of Stark states decreases with increasing electric field leading to reduced hopping probability and a region of negative differential conductivity (NDC).<sup>2,9</sup>

When a magnetic field is applied in the superlattice direction magnetic quantization leads to the formation of Landau levels which facilitates a series of resonances in the conduction process caused by the interplay of the Bloch and cyclotron frequencies. Most notably Stark cyclotron resonance (SCR)<sup>10</sup> has been observed when Landau-Stark ladder states are isoenergetic allowing elastic scattering processes to occur when

$$\delta\nu \hbar \Omega = \delta n \hbar \omega_c, \quad (1)$$

where  $\omega_c$  is the cyclotron frequency, and  $\delta\nu$  and  $\delta n$  are integers. The resulting increased current relies on energy loss due to relaxation between the Landau levels within individual wells. Some examples of Stark cyclotron resonance have been reported<sup>10,11</sup> although the effect is not particularly strong due to the limited energy loss processes.

Theoretical treatments also predict Stark cyclotron phonon resonance<sup>12,13</sup> (SCPR) to occur under the condition

$$\delta\nu \hbar \Omega = \delta n \hbar \omega_c \pm \hbar \omega_{LO}, \quad (2)$$

where  $\hbar\omega_{LO}$  is the longitudinal optical (LO) phonon energy, due to the enhancement of energy loss from the very strongly coupled LO phonon mode. This emission has been predicted to be resonantly enhanced at the Stark magnetophonon

(SMPR) condition<sup>14</sup> where the SCR is resonantly enhanced by fast emission of  $\delta N$  LO phonons. SMPR is predicted to occur under the condition

$$\delta\nu \hbar \Omega = \delta n \hbar \omega_c = \delta N \hbar \omega_{LO}. \quad (3)$$

Reports of SMPR in type-I GaAs/AlGaAs (Ref. 15) have been made, which demonstrate that resonance occurs at the fundamental SMPR condition ( $\delta n = \delta N = 1$ ). In this paper we report multiple resonances in the type-II InAs/GaSb system<sup>16,17</sup> which has a low carrier effective mass allowing study of transport at cyclotron energies considerably above the LO phonon energy ( $\hbar\omega_{LO} = 30$  meV). Samples are grown with narrow InAs wells such that no overlap exists between electron and hole states. Despite this tunnelling between adjacent superlattice layers is dominated by interband coupling and is strongly  $\mathbf{k}$  dependent. Reduced tunnelling in higher energy Landau level minibands (LLMBs) promotes sequential transport in this system and suppresses electric field domain formation, allowing a much clearer demonstration of the role of resonant energy loss processes. One further consequence of this is that a magnetic field applied parallel to the superlattice growth direction also causes a reduction of interband coupling and results in progressively narrower miniband widths<sup>18</sup> at higher magnetic fields and for higher Landau levels.

Experiments were performed on 100 period undoped InAs/GaSb superlattices grown using an MOVPE reactor. Samples were grown on *n*-type InAs substrates with 5000 Å InAs buffer and cap layers. The ratio of InAs/GaSb ( $R$ ) is estimated from MOVPE growth rates measured using an *in-situ* surface photoabsorption technique.<sup>19</sup> Samples were also characterized using x-ray diffraction (XRD) which gave accurate values of the superlattice period ( $d$ ).

Direct characterization of the superlattice band structure was performed using FTIR magnetoabsorption spectroscopy to measure the superlattice band gaps. This was compared with  $\mathbf{k} \cdot \mathbf{p}$  simulations<sup>20</sup> used to calculate the band structure. The results were used to refine estimates of the ratio  $R$  and show that miniband width estimates in Table I are correct to within an error of  $\pm 15\%$ . Sample characteristics are summarized in Table I. The superlattice band structure calculations show that there is a large minigap ( $\sim 300$  meV) between minibands. Higher minibands can therefore be expected to

TABLE I. Sample characteristics.

Sample No.	$d$ (Å) <sup>a</sup>	$R$ ( $d_{\text{InAs}}/d_{\text{GaSb}}$ ) <sup>b</sup>	$\Delta$ (meV)	$p$
4572	134	0.37	7	55
4570	126	0.34	12	63
4561	126	0.50	13	59
4579	117	0.63	27	62
3756	93	0.82	48	67

<sup>a</sup>Measured with XRD.

<sup>b</sup>Estimated with SPA data.

<sup>c</sup>Estimated using  $\mathbf{k} \cdot \mathbf{p}$  calculations ( $\pm 15\%$  error).

play no role within the electric field ranges studied in this paper.

For vertical transport measurements 150  $\mu\text{m}$  mesas were defined using standard lithographic and wet etching techniques.  $I(V)$  measurements in magnetic fields up to 19.5 T were performed using an Oxford Instruments superconducting magnet. Measurements were performed at  $T=20$  K in a VTI to avoid magnetic freeze-out of the  $n$ -InAs substrate affecting the observed resonance positions.

Figure 1 shows the  $I(V)$  characteristics for sample 4572 at  $B=0-19.5$  T and  $T=20$  K.  $I(V)$  curves at  $B=0$  T display a linear transport regime up to  $\sim 300$  mV followed by a resonant transport feature at  $\sim 400$  mV (identified as a shoulder and plateau), in good agreement with conventional Esaki-Tsu miniband transport theory.<sup>2</sup>

At high bias a further resonant transport peak is observed at  $\sim 2000$  mV and attributed to electron-phonon resonances in the Stark hopping regime. Theoretical investigation of this effect has been reported by a number of groups<sup>21,22</sup> who predict LO phonon mediated hopping conduction in a uniform WSL when conditions satisfy

$$\delta\nu \hbar \Omega = \hbar \omega_{\text{LO}}, \quad (4)$$

where electrons tunnel through  $\delta\nu$  superlattice wells followed by the emission of an LO phonon to a lower energy

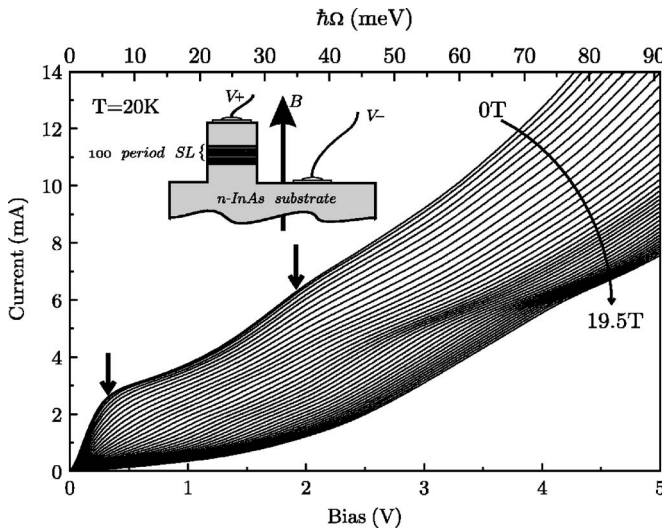


FIG. 1.  $I(V)$  characteristic for sample 4572,  $\Delta_{n=0}(0)=7$  meV and  $T=20$  K. Inset displays a schematic of the sample geometry.

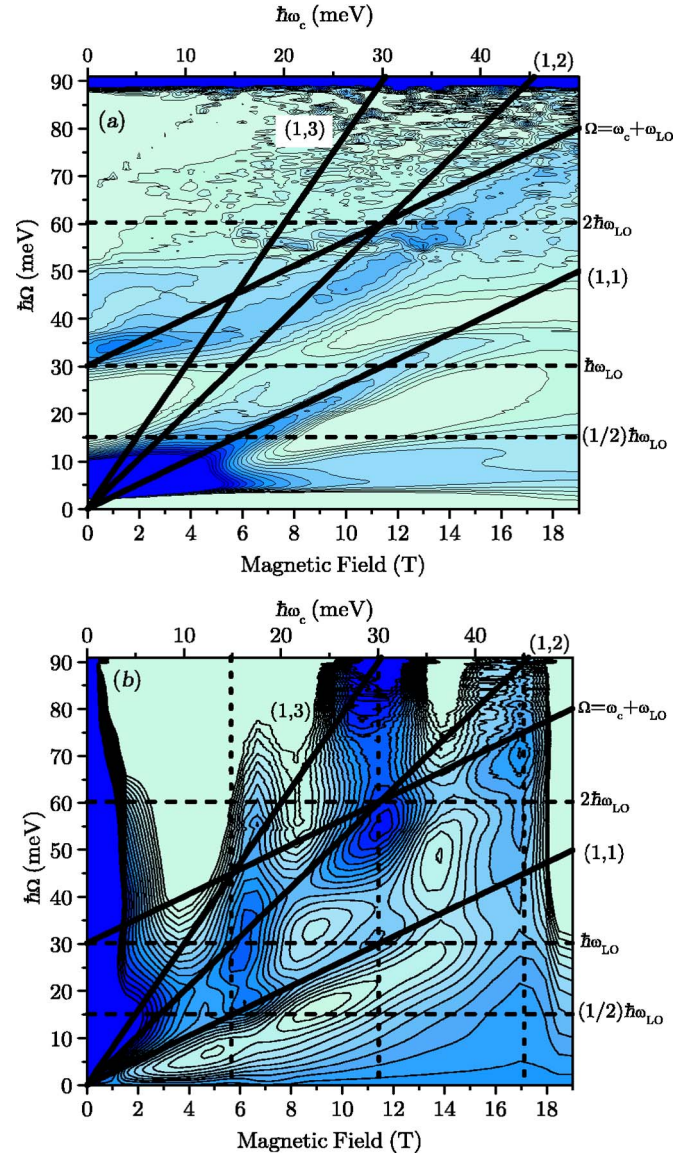


FIG. 2. (Color online) Sample 4572  $\Delta_{n=0}(0)=7$  meV  $p=55$  and  $m^*=0.044$ . (a) Plot of  $-d^2I/dV^2$ . (b) Plot of  $-d^2I/dB^2$ . In both color scales dark and light shades represent plot maxima and minima, respectively.

WSL state. Samples display no domain formation within the bias regime studied (0–5 V), indicating that the sequential transport picture in a uniform field is appropriate.

It is apparent from Fig. 2(a) that increasing  $B$ -field causes a suppression of the WSL Stark phonon resonance feature at  $\hbar\Omega \sim 30$  meV ( $\sim 2000$  mV). The increasing magnetic field decouples the vertical and lateral (in-plane) superlattice transport and restricts the possible elastic scattering transitions. Increasing  $B$  field thus suppresses WSL hopping transport due to the transition to the quantum box SL regime.<sup>23,24</sup>  $I(V)$  characteristics at high  $B$  field display a strong magnetoresistance which is of order of 100 times greater than observations in type-I systems.<sup>23</sup> The strong magnetoresistance is an indication of the importance of total quantization in the InAs/GaSb system.

Plots of  $-d^2I/dV^2$  and  $-d^2I/dB^2$  are used to highlight the

interaction of the Bloch and cyclotron frequencies in the WSL transport regime. Negative second derivative plots remove the monotonic background resistance, show maxima in conductance and allow the observation of weak resonances. Results of such analysis are presented as contour plots with gray scales selected to display maxima which identify areas of high conductivity. Plots of  $-d^2I/dV^2$  and  $-d^2I/dB^2$  are sensitive to resonances which vary with  $V$  and  $B$ , respectively. Contour plots are presented in Fig. 2 for sample 4572. Note that the contour plots are generated from the same set of data transposed and reanalyzed. As the  $B$  field increases a series of resonances caused by the interplay of the cyclotron and Bloch frequencies are observed.

At fields above  $\sim 4$ T plots of  $-d^2I/dV^2$  are dominated by peaks attributed to SCR and fitted with Eq. (1) using indices  $(\delta\nu, \delta n)$  and  $m^*$ . An effective mass of approximately  $0.05m_e$  is predicted by  $\mathbf{k} \cdot \mathbf{p}$  calculations for the superlattice transport regime and agreement with this value in the WSL regime is found from the magnetophonon resonances (MPR) discussed below. Fits of the Bloch frequency for the SCR condition require a lower number of active periods ( $p$ ) than the nominal 100 grown (the number of active periods for each sample is given in Table I). Low temperature magnetotransport reveals 2D Shubnikov de Haas oscillations with  $n_D \sim 10^{12} \text{ cm}^{-2}$ , due to the formation of a 2D electron accumulation layer at the substrate-superlattice and superlattice-cap interfaces which causes an increased tunnelling probability and subsequently higher conductivity in the first and last periods of the structure.

All of the samples studied reveal a range of SCR transitions with indices  $(\delta\nu, \delta n)$  equal to (1,1) and (1,2) and (1,3). In addition the samples with larger miniband widths also show a (2,1) resonance, due to the increased hopping probability which allows tunnelling between next nearest neighbors. The SCR peaks are stronger than those observed by Canali *et al.*<sup>10</sup> in type-I GaAs/AlGaAs superlattices in the low field range  $B=0-9.2$  T, but show fewer high order features. This is due to the extreme localization and reduced hopping probability for higher energy states within the InAs/GaSb SL quantum wells due to reduced interband mixing at higher energies. The SCR resonances become steadily stronger with field as also observed by Canali *et al.*<sup>10</sup> but then weaken rapidly once the SMPR condition (3) has been reached. This suggests that the processes of energy loss are strongly suppressed once the Bloch frequency becomes larger than the LO phonon energy.

The above behavior demonstrates that satisfying the SCR condition alone does not result in a significant transport current unless there is an energy dissipation process to create a net electron flow. This role is typically filled by acoustic phonon emission at low fields, but at high bias the most efficient dissipative process available is LO phonon emission. In the high  $B$ -field WSL hopping regime LO phonon emission is only possible when electrons can reach a state which satisfies condition (3), due to the discrete WSL energy spectrum and constant LO phonon energy.

To achieve resonance an electron is required to tunnel through  $\delta\nu$  periods of the superlattice into a higher WSL Landau level, gaining potential energy  $\delta N \hbar \omega_{LO}$ , before LO

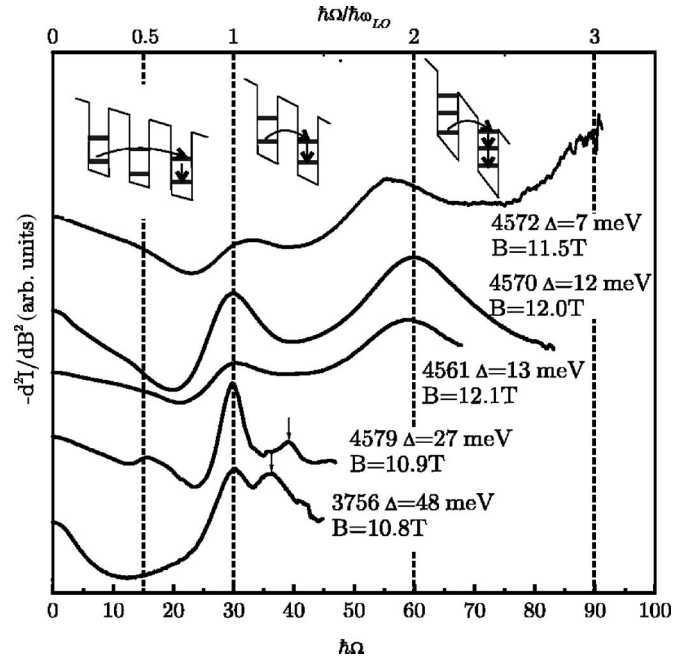


FIG. 3. Plot of  $-d^2I/dB^2$  as a function of  $\hbar\Omega$  at the  $\delta n=1$  MPR condition for samples 4572, 4570, 4561, 4579, and 3756. The curve for sample 4572 is extracted from Fig. 2(b). Inset diagrams display the Wannier-Stark Landau level alignment and LO phonon relaxation processes for each fitted feature.

phonon emission is possible. Successive tunnelling into higher WSL Landau levels in the InAs/GaSb system is however strongly suppressed.<sup>18</sup> The probability of LO phonon emission processes is therefore very small for large  $\delta\nu$ , thus requiring  $\delta n$  and  $\delta N$  to be small.

Plots of  $-d^2I/dB^2$  are much more sensitive to processes which are resonant in magnetic field as can be seen from Fig. 2(b). This shows strong magnetophonon resonances at both the fundamental,  $\delta n=1$ , resonance and the  $\delta n=2$  harmonic (identified at  $B=11.5$  T and  $B=6$  T in sample 4572). In addition the vertical line at  $B=17$  T corresponds to the  $(\delta n=2, \delta N=3)$  resonance. All of these resonance conditions are consistent with an effective mass of  $m^* = 0.045 \pm 0.002 m_e$ . Conduction shows field dependent peaks for all bias fields, but there is an additional enhancement when the SCR conditions are coincident with the MPR resonance. For example, the increased intensity at  $\hbar\Omega=55$  meV and  $\hbar\Omega=30$  meV where  $B=11.5$  T.

Good fits to Eq. (3) are observed for the  $\delta n=1, 2$  MPR when coincident with the (1,1), (1,2), and (1,3) SCR. At these points a triple resonance occurs and the Landau level ladder provides a sequence of resonant intermediate states which results in a much larger enhancement of transport current at magnetic fields given by the SMPR Eq. (3). This behavior is described in the predictions of Mori *et al.*<sup>14</sup> for type-I superlattice systems and the observed features in Fig. 2 display remarkable qualitative agreement with the theory.

The triple (SMPR) resonances are shown in Fig. 3 where  $-d^2I/dB^2$  is plotted as a function of the Bloch frequency  $\hbar\Omega$  at the magnetic field corresponding to the  $\delta n=1$  MPR conditions for all of the samples studied, covering miniband



widths from 7 to 48 meV. The resonances are particularly enhanced for the Stark phonon condition given by Eq. (4) thus providing proof of the triply resonant condition. The resonances become progressively stronger as the bias increases (although the highest biases could not be studied in the wider minibandwidth samples due to the high current levels). This suggests that the phonon emission processes are dominated by resonant transitions within a single well. This could then lead to optic phonon amplification as has been suggested recently for acoustic phonons.<sup>26</sup> The highest  $\Delta$  samples also show the appearance of a second peak just above the main SMPR condition which is thought to be due to the appearance of interwell emission, which will be shifted from the intrawell emission by a tunnelling energy equivalent to the miniband (Esaki-Tsu) transport peak ( $\hbar\Omega=5-10$  meV in the current samples).

At cyclotron energies above the fundamental ( $\delta n=1$ ) MPR we observe that the (1,2) resonance is replaced with a SCPR feature [Eq. (2)], described by the condition  $\Omega=\omega_c+\omega_{LO}$ . At high  $\omega_c>\omega_{LO}$  intrawell LO phonon relaxation is forbidden by the large cyclotron energy gap. Interwell transitions in which an electron tunnels and emits an LO phonon then make an increasingly dominant contribution to the

transport characteristics. Under these conditions it has been suggested that ordered domain structures may begin to occur<sup>25</sup> in order to optimize the overall tunnelling probability.

In summary, we have performed magnetotransport measurements of strongly coupled InAs/GaSb superlattice with a range of miniband widths. The application of high electric and magnetic fields causes total quantization of the electronic states and conduction becomes dominated by resonant tunnelling and energy emission processes. Stark cyclotron resonance caused by elastic interwell tunnelling is found to be dramatically enhanced when combined with resonant intrawell energy emission processes, leading to the observation of the triple Stark magnetophonon resonance. The observation of strong high order SMPR peaks demonstrates that the LO phonon emission is predominantly an intrawell process. Some evidence for interwell LO phonon emission is found for high  $\Delta$  samples and away from the MPR condition. Overall it is demonstrated that magnetic fields can be used to investigate high electric field conduction in superlattices, probing the role of interwell and intrawell tunnelling in elastic and inelastic processes.

\*Electronic address: r.deacon1@physics.ox.ac.uk

<sup>1</sup>A. Wacker, Phys. Rep. **357**, 1 (2002).

<sup>2</sup>L. Esaki and R. Tsu, IBM J. Res. Dev. **14**, 61 (1970).

<sup>3</sup>H. J. Hutchinson, A. W. Higgs, D. C. Herbert, and G. W. Smith, J. Appl. Phys. **75**, 320 (1994).

<sup>4</sup>A. Sibille, J. F. Palmier, H. Wang, and F. Mollot, Phys. Rev. Lett. **64**, 52 (1990).

<sup>5</sup>R. Tsu and L. Esaki, J. Appl. Phys. **43**, 5204 (1991).

<sup>6</sup>E. E. Mendez, F. Agulló-Rueda, and J. M. Hong, Phys. Rev. Lett. **60**, 2426 (1988).

<sup>7</sup>M. Kast, C. Pacher, G. Strasser, E. Gornik, and W. S. M. Werner, Phys. Rev. Lett. **89**, 136803 (2002).

<sup>8</sup>R. Tsu and G. Dohler, Phys. Rev. B **12**, 680 (1975).

<sup>9</sup>F. Beltram, F. Capasso, D. L. Sivco, A. L. Hutchinson, Sung-Nee G. Chu, and A. Y. Cho, Phys. Rev. Lett. **64**, 3167 (1990).

<sup>10</sup>L. Canali, M. Lazzarino, L. Sorba, and F. Beltram, Phys. Rev. Lett. **76**, 3618 (1996).

<sup>11</sup>J. Liu, E. Gornik, S. J. Xu, and H. Z. Zheng, Semicond. Sci. Technol. **12**, 1422 (1997).

<sup>12</sup>N. H. Shon and H. N. Nazareno, Phys. Rev. B **53**, 7937 (1996).

<sup>13</sup>P. Kleinert and V. V. Bryksin, Phys. Rev. B **56**, 15827 (1997).

<sup>14</sup>N. Mori, C. Hamaguchi, L. Eaves, and P. C. Main, Physica B **298**, 329 (2001).

<sup>15</sup>D. Fowler, A. Patané, A. Ignatov, L. Eaves, M. Henini, N. Mori,

D. K. Maude, and R. Airey, Appl. Phys. Lett. **88**, 52111 (2006).

<sup>16</sup>G. A. Sai-Halasz, R. Tsu, and L. Esaki, Appl. Phys. Lett. **30**, 651 (1977).

<sup>17</sup>G. A. Sai-Halasz, L. Esaki, and W. A. Harrison, Phys. Rev. B **18**, 2812 (1978).

<sup>18</sup>V. J. Hales, A. J. Poulter, and R. J. Nicholas, Physica E (Amsterdam) **7**, 84 (2000).

<sup>19</sup>P. C. Klipstein, S. G. Lyapin, N. J. Mason, and P. J. Walker, J. Cryst. Growth **195**, 168 (1998).

<sup>20</sup>G. Bastard, Phys. Rev. B **24**, 5693 (1981).

<sup>21</sup>A. O. Govorov and M. V. Èntin, Solid State Commun. **92**, 977 (1994).

<sup>22</sup>V. V. Bryxin and Y. A. Firsov, Solid State Commun. **10**, 471 (1971).

<sup>23</sup>A. Patané, N. Mori, D. Fowler, L. Eaves, M. Henini, D. K. Maude, C. Hamaguchi, and R. Airey, Phys. Rev. Lett. **93**, 146801 (2004).

<sup>24</sup>A. B. Henriques, R. S. Deacon, and R. J. Nicholas, Braz. J. Phys. **32**, 605 (2004).

<sup>25</sup>R. S. Deacon, R. J. Nicholas, A. B. Henriques, and N. J. Mason, Photonics Spectra **22**, 316 (2004).

<sup>26</sup>A. J. Kent, R. N. Kini, N. M. Stanton, M. Henini, B. A. Glavin, V. A. Kochelap, and T. L. Linnik, Phys. Rev. Lett. **96**, 215504 (2006).